

The analysis and performance of large-scale stand-alone solar desalination plants

P.T. Tsilingiris

Center for Renewable Energy Sources (CRES), 19 km Marathon Avenue, 190 09 Pikermi, Attiki, Greece

Received 16 January 1995; accepted 20 March 1995

Abstract

The development of a simple dynamic computer model allows the performance and operational behavior investigation of a large solar seawater desalination system based on a multi-effect distillation plant and a solar pond, which is believed to be the most promising large-scale solar desalination technology known today. The whole system of dynamic behavior of the whole system is investigated, and annual water yield predictions are made during the thermal transient build-up and quasi-steady-state system operation. The effect of various design and operational parameters on system behavior are investigated. Results are offered for system sizing, design and water yield predictions, as well as system economic evaluation. Based on up-to-date construction experience, rates and market costs of components and labor, as well as updated costs of commercially available desalination plants, predictions of the unit water cost are made according to which appears to be most competitive with water cost from conventional resources in several arid and semi-arid geographical locations.

Keywords: Solar desalination; Multi-effect distillation; Solar ponds

1. Introduction

Water is one of the most basic requirements of all mankind. The evolution of human civilization has been based for centuries on adequate fresh groundwater deposits of reliable supply from distant fresh water sources. However, the shortage of fresh water is gradually spreading at alarming levels, even in the temperate climate zones on earth, probably due to recent environmental pol-

lution and global warming, which strongly affects the hydrological cycle on earth. Large-scale sea or brackish water desalination, although an energy-intensive process, appears to be the solution which is being offered by contemporary technology. However, the ever-rising costs of conventional energy and the increasing concern to regional and global environmental pollution are leading to the exploitation of environmentally friendly and low-cost solar energy.

2. Large-scale solar pond-multi-effect distillation technology

Thermal desalination processes involving a large number of successive brine evaporation-condensation cycles with intermediate heat recovery are currently considered as the most suitable for large-scale desalination plants with high salinity (up to 40,000 ppm) water sources. These units, based either on multi-effect distillation (MED) or the multi-stage flash (MSF) principle, can be operated by low-grade heat sources (usually above 65°C) with a specific heat consumption as low as 64 kWh (thermal) per ton of distillate. They are currently manufactured in medium and large capacities up to several thousand tons of distillate daily. When there are no site restrictions present, the units can be operated by large conventional medium temperature solar collector fields.

Due to the extremely large amounts of low-grade heat required for the processes, the units require enormous fields of conventional solar collectors. However, construction and operation of such enormous collector fields are impractical taking into account the associated interconnection plumbing and thermal insulation, flow balance, maintenance, heat storage and pumping, as well as capital costs. A potential device which is suitable for this purpose is the salinity gradient solar pond (SP), which not only involves adequate integral heat storage and passive heat collection and transfer at low pumping costs but also can be built and operated at a remarkably low cost.

Large-scale solar seawater desalination technology has received considerable attention during the last two decades. Tabor [1] found that when suitable site conditions for erection of large low-cost SP and MED plants exist, this technology will be cost effective. Considerable amounts of expertise and practical experience have been gained on both salinity gradient SP and MED plants in Israel and elsewhere [2-4], while large MED plants are currently manufactured by several companies around the world.

3. Description of the theoretical model

The present work aims at the development of a simple theoretical computer model for the investigation of the dynamic behavior of a combined large SP-MED system. Based on the literature and mainly on specific information by Zarza et al. [5] for a currently manufactured, small-capacity (about 80 m³/d), 14-stage, MED desalination plant with a specific heat consumption of 75 kWh thermal/m³, it appears as though that even lower figures could be expected for appreciably higher plant capacities.

It is assumed that a 500 m³/d MED plant is combined with a large SP as a low-grade heat source, which supplies heat to the plant as soon as its lower convecting zone (LCZ) temperature exceeds 75°C. Edge effects are ignored while a fixed temperature heat sink is assumed at 8 m underneath the pond bottom. It has been recently found [6] that due to the substantial amplitude of harmonic meteorological driving functions for latitudes higher than about 25°N and to the relatively limited thickness of practically feasible GZ according to Xe et al. [7] and Tsilingiris and Mullett [8], dynamic modelling formulation is necessary since steady-state formulation may possibly lead to highly misleading results. The heat flow in the brine and soil are described, respectively, from the following expressions:

$$\rho_b \cdot c_b \cdot \frac{\partial T_b(x,t)}{\partial t} = \frac{\partial}{\partial x} \cdot \left[k_b \cdot \frac{\partial T_b(x,t)}{\partial x} \right] - \frac{\partial H_0(t)}{\partial x} \cdot (1-l) \cdot h(x) \quad (1)$$

$$\rho_s \cdot c_s \cdot \frac{\partial T_s(x,t)}{\partial t} = \frac{\partial}{\partial x} \cdot \left[k_s \cdot \frac{\partial T_s(x,t)}{\partial x} \right] \quad (2)$$

where \bar{l} is the dimensionless yearly average Fresnel optical loss coefficient while the final term of Eq. (1) represents the heat generation due to the absorption of incident solar energy. Al-

though it has been found that the theoretical upper limit for brine transparency would be expected to be appreciably higher [9], the radiation transmission in this model is assumed to follow the more conservative simple Bryant and Colbeck [10] law:

$$h(x) = a + b \ln(x/\cos\bar{\theta}) \quad (3)$$

with $\bar{\theta}$ the average refractive angle for the actual path length correction according to Rabl and Nielsen [11], assumption and H_0 the incident solar radiation harmonic function. Brine and soil are subdivided into discrete isothermal layers, and the above equations are translated into corresponding heat balance expressions. They are solved simultaneously under the boundary conditions of pond surface and underground heat sink layer equal to daily ambient and average yearly temperature, respectively, and the following lower convecting layer balance expression,

$$\begin{aligned} \rho_b \cdot c_b \cdot (x_3 - x_2) \cdot \frac{\partial T_b(x,t)}{\partial t} \\ - k_b \cdot \frac{\partial T_b(x,t)}{\partial x} \Big|_{x=x_2} - k_s \cdot \frac{\partial T_s(x,t)}{\partial x} \Big|_{x=x_3} \\ + (1 - \bar{l}) \cdot H_0(t) \cdot h(x_2) - L(x_2, t) = 0 \end{aligned} \quad (4)$$

where x_1, x_2, x_3, x_4 are the vertical distances from the surface of the pond to the lower boundaries of UCZ, GZ, pond bottom and heat sink, respectively. As soon as LCZ temperature exceeds 75°C, the MED plant, which is assumed to withstand slight overloads of up to 120% of its rated nominal capacity during relatively short periods of time, operates at a fixed temperature with a distillate production within period Y given by

$$M_Y = \int_0^Y [A_c \cdot L(x_2, t) / w] \cdot dt \quad (5)$$

4. Results and discussion

It is assumed that the combined system begins operation in spring at day $N=100$ when brine and soil are isothermal. Fig. 1 shows the LCZ temperature as a function of time in days during the period of the first three successive years of operation. Calculated results correspond to an UCZ, GZ and LCZ of 0.2, 1 and 1.5 m thick, respectively, a pond area of 30,000 m², and meteorological conditions corresponding to Athens (38°N latitude). Within the first 100 days, LCZ temperature exceeds the extraction temperature and the MED plant becomes operational. Calculated daily water production is shown by the solid lines during which each of these curves corresponds to the yearly water production. Distillate production ceases as soon as LCZ temperature becomes lower than 75°C. During the first two years of operation, water production increases substantially and stabilizes from the third year onwards when the system approaches quasi-steady-state periodic solutions and all transients have died away. This long transient behavior is attributed to the substantial thermal inertia of the system. Based on extensive computer simulations, it has been recently found [6] that for the given geographical region, it can be assumed that the system practically reaches quasi-steady-state conditions after the end of the second operating year, irrespective of design and operational pond characteristics. In the same plot the broken lines underneath the solid line represent the ratio of the distillate production to the daily nominal capacity. This capacity ratio never exceeds about 1.2, something which suggests a fairly good match between the pond and MED plant.

Fig. 2 represents the dynamic behavior of the combined SP-MED plant during a whole year when all transients have died away. The broken line corresponds to the LCZ temperature, and solid lines correspond to daily water production for an UCZ, GZ, and an LCZ of 0.2, 1 and 1.5 m, respectively, and a pond area of 10,000, 20,000, and 30,000 m². Apparently best-capacity match-

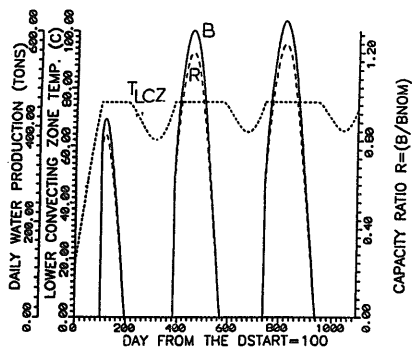


Fig. 1. The LCZ temperature, T_{LCZ} , daily water yield B and daily water yield and capacity ratio R during the first three successive operating years. UCZ thickness=0.2 m, GZ thickness=1 m, LCZ thickness=1.5 m.

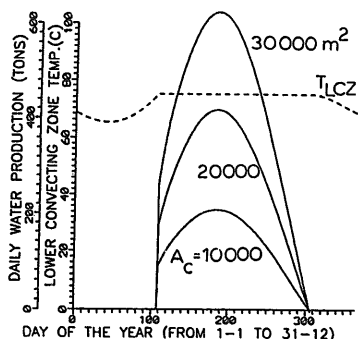


Fig. 2. Quasi-steady-state LCZ temperature (broken line) and daily water yield (solid line) for $A_c=10,000$, $20,000$, and $30,000$ m² and UCZ thickness=0.2 m, GZ thickness=1.0, and LCZ thickness=1.5 m.

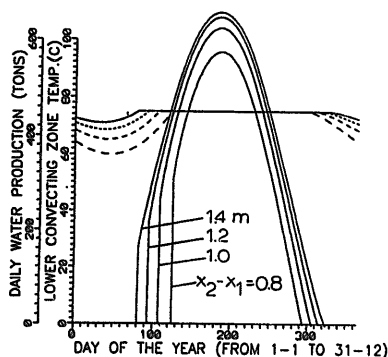


Fig. 3. The effect of GZ thickness of 0.8, 1, 1.2 and 1.4 m on LCZ temperature and water yield in quasi-steady-state operation for a GZ thickness of 0.2 m and an LCZ thickness of 1.5 m.

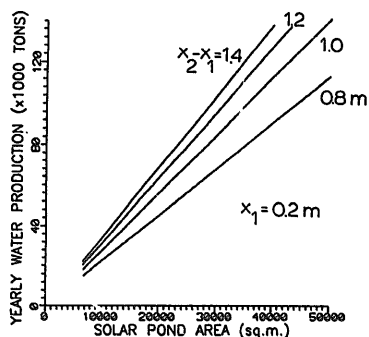


Fig. 4. The yearly water production as a function of solar pond area with the GZ thickness as a parameter and UCZ thickness of 0.2 m and LCZ thickness of 1.5 m.

ing is possible with about a 30,000 m² pond size, while water production is possible between about day 110 to 310 yearly.

Fig. 3 represents the effect of a practically feasible GZ thickness of 0.8, 1, 1.2 and 1.4 m on the daily water production under similar operating conditions. Although highly desirable, it is not

feasible to design thicker gradient zones with the widely available brines.

Apparently the effect of GZ is not only remarkable to the yearly water production, which is proportional to the surface underneath each curve, but also to the operational period of the combined SP-MED plant, which increases from 170 to 245 d yearly corresponding to a GZ of 0.8-1.4 m, respectively.

In Fig. 4 the yearly water production is plotted as a function of solar pond area with the GZ thickness between 0.8-1.4 m, under the assumption of negligible edge effect losses. These results can be used as a rough SP dimensioning chart for operation of SP-MED plants in a typical sunny Mediterranean climate.

5. Economic analysis

The overall capital cost is mainly composed of the solar system cost and MED plant cost components. According to the most reliable and up-to-date SP construction experience, Nielsen [12] has estimated the SP unit cost as a function of many parameters. The unit cost area of a solar pond also shown in [13] is expressed as a contribution of the SP and evaporation pond components. These are expressed as a function of earth moving, polymer liner, wind protection, load heat exchanger and the salt unit cost, which dominates. However, when pond erection is possible along coastal areas for seawater desalination applications, salt can simply be derived by seawater concentration in shallow evaporating ponds at a negligible cost.

Cost estimates for large, modern, commercially available desalination plants are rather scarce and sometimes not current, and direct access to manufacturing companies is usually difficult. However, it is generally agreed that their cost is a linear function of their nominal capacity:

$$C = \alpha + \beta \cdot B_n \quad (6)$$

with α and β numerical constants. The capacity-dependent cost component is usually assumed

proportional to the number of plant stages or effects.

Based mainly on the current market costs of substantially smaller capacity desalination plants, it has been found that the numerical figures of the capacity-dependent and independent terms β and α , respectively, scatter substantially, with maximum figures as high as \$2500/m³/d and \$200,000, respectively. However, since some of these figures correspond to research plants, they cannot be considered as representative, and they cannot be directly extrapolated for large- and very large-capacity plants, the cost for which is expected to drop substantially with size.

Tabor [1] assumes for large-capacity plants that $\beta = \$700 \text{ m}^3/\text{d}$. Based on this estimate and updating this figure, taking into consideration typical inflation rates as well as design and engineering improvements along with innovative technology, it could be very reasonable to assume for large-capacity plants that $\beta = \$1,000/\text{m}^3/\text{d}$. Therefore, in order to present a sample case for use in the developed model and although the original figures correspond to earlier cost estimates, the following figures of $\alpha = \$50,000$ and $\beta = \$1000 \text{ m}^3/\text{d}$ have been adopted for the subsequent economic analysis.

Although economically desirable, continuous operation of the MED plant is impossible throughout the year because of necessary preventive maintenance of the plant. Defining as maintenance factor MF , the percentage of the uninterrupted plant operation yearly and assuming that $MF = 80\%$, the yearly average derating factor is

$$\bar{R} = M_Y / 365 \cdot B_n \cdot MF \quad (7)$$

and the effective plant cost is estimated as

$$C_d = C_n / \bar{R} = 365 \cdot MF \cdot B_n \cdot C_n / M_Y \quad (8)$$

For a given zone geometry, the yearly water production as a function of SP area is given in Fig. 4. Assuming a gradient zone of 1 m thick, the yearly water production is estimated by

$$B_y = 0.002825 \cdot A_c \quad (9)$$

Therefore, the overall cost of the SP plus MED plant is given by

$$C_o = sc_p \cdot A_c + 129.2 \cdot MF \cdot C_n \cdot B_n / A_c \quad (10)$$

which becomes minimum for $(\partial C_o / \partial A_c) = 0$.

The overall capital cost of a solar pond and a MED plant is shown in Fig. 5 as a function of SP area with the unit salt cost as a parameter ranging from \$0-60/ton. It is shown that for a salt cost of \$60/ton a minimum capital cost of about \$2 million is possible for a pond area of about 30,000 m², which leads to more than 80,000 tons of yearly water production. Apparently the expensive component of the system is the MED plant, the commercial cost of which is expected to fall with market growth and technological improvements.

Assuming a 15-y life span and referring to annual costs, it would be possible to estimate the produced water unit cost. In Fig. 6 the water cost is shown as a function of a solar pond area for salt costs of \$0, \$20, \$40 and \$60/ton with annual

interest rates of 6% and 14%. Apparently the effect of interest rates on cost dominates at smaller installations, while water cost is estimated to be slightly in excess of \$2/ton for a pond of about 30,000 m², which matches with the given size of the MED plant.

6. Conclusions

An analysis of a stand-alone SP-MED for seawater desalination and an economic evaluation of the technology have been presented. The development of a theoretical computer model and dynamic formulation has allowed the complete investigation of design and operational parameter effects on the distillate production of a combined, stand-alone SP-MED seawater desalination plant. Derived transient and quasi-steady-state solutions were used for the calculation of yearly water production as a function of pond area during the first and subsequent years of operation, as well as the yearly operational period of the plant for a fixed zone configuration.

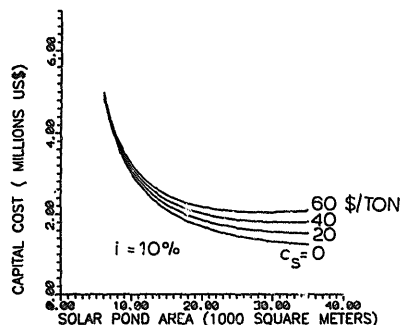


Fig. 5. Capital cost for the whole SP-MED plant system as a function of solar system size with unit salt cost as a parameter. It is assumed that UCZ thickness is 0.2 m, GZ thickness 1.0 m, and LCZ thickness 1.5 m, with an interest rate $i=10\%$.

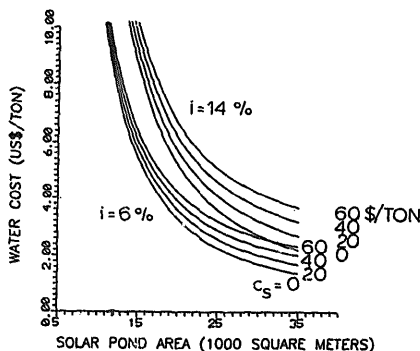


Fig. 6. Water cost as a function of solar system area with unit salt cost and interest rate as parameters ranging from \$0-60/ton and from 6-14%, respectively. The UCZ thickness is 0.2 m, GZ thickness 1.0 m and LCZ thickness 1.5 m.

It has been found that a system based on a pond area of 30,000-40,000 m² under meteorological conditions of a sunny Mediterranean country is capable of delivering about 100,000 tons of distilled water (about 10 ppm) yearly at a cost of slightly in excess of \$2/m³, which is competitive with the cost of water from conventional water resources for many other arid and semi-arid locations.

7. Symbols

<i>a</i>	— numerical constant
<i>A</i>	— area, m ²
<i>b</i>	— numerical constant
<i>B</i>	— MED plant capacity, m ³ /d
<i>c</i>	— heat capacity, J/Kg°C
<i>C</i>	— cost, \$
<i>h</i>	— transmission function
<i>H</i>	— incident solar radiation, w/m ²
<i>k</i>	— thermal conductivity, w/m°C
\bar{T}	— yearly average optical loss coefficient
<i>L</i>	— heat extraction rate, w/m ²
<i>M</i>	— distillate production, kg
<i>MF</i>	— maintenance factor
<i>R</i>	— capacity ratio
<i>sc</i>	— specific cost, \$/m ²
<i>T</i>	— temperature
<i>t</i>	— time
<i>w</i>	— specific heat consumption of the MED plant, J/kg
<i>x</i>	— depth, m
<i>Y</i>	— time period ^d , s

Greek

α	— numerical constant
β	— numerical constant
$\bar{\theta}$	— average refractive angle
ρ	— water density, kg/l

Subscripts

<i>b</i>	— brine
<i>c</i>	— solar collection
<i>d</i>	— effective
<i>n</i>	— nominal
<i>o</i>	— overall
<i>p</i>	— pond
<i>s</i>	— soil
<i>Y</i>	— time period, y

References

- [1] H. Tabor, *Desalination*, 17 (1975) 289.
- [2] A.H.P. Swift, R.L. Reid and K.D. McGraw, in: *Proc. ASME, Denver, 1988*, pp. 107-112.
- [3] G. Caruso, A. Moriconi and A. Naviglio, in: *Proc. 2nd Intern. Conf. Progress in Solar Ponds, Rome, 1990*, pp. 491-497.
- [4] H. Tabor and B. Doron, in: *Proc. 1st Intern. Conf. Progress in Solar Ponds, Cuernavaca, Mexico, 198*, pp. 206-212.
- [5] E. Zarza, J. Ajona, J. Leon, K. Genter and A. Gregorzewski, in: *Proc. ISES Intern. Congress, Denver, 1991*, pp. 2270-2275.
- [6] P.T. Tsilingiris, *Solar Energy*, 53 (1994) 73.
- [7] H. Xe, P. Golding and C.E. Nielsen, in: *Proc. 1st Intern. Conf. Progress in Solar Ponds, Cuernavaca, Mexico, 1987*, pp. 107-117.
- [8] P.T. Tsilingiris and L.B. Mullett, *Energy Res.*, 13 (1989) 527.
- [9] P.T. Tsilingiris, *Solar Energy*, 40 (1988) 41.
- [10] H.C. Bryant and J. Colbeck, *Solar Energy (Techn. Note)*, 19 (1977) 321.
- [11] A. Rabl and C.E. Nielsen, *Solar Energy*, 17 (1975) 1.
- [12] C.E. Nielsen, in: *Advances in Solar Energy*, K.W. Boer, ed., Plenum Press, New York, 1988.
- [13] P.T. Tsilingiris, *Solar Energy*, 49 (1992) 19.